Available online at www.sciencedirect.com
ScienceDirect
Journal of Solid State Chemistry 180 (2007) 440–445
JOURNAL OF SOLID STATE CHEMISTRY
www.elsevier.com/locate/jssc

Metal valences in electron-doped $(Sr,La)_2FeTaO_6$ double perovskite: A ^{57}Fe Mössbauer spectroscopy study

E.-L. Rautama[a,b], J. Lindén[c], H. Yamauchi[a], M. Karppinen[a,b,*]

[a] *Materials and Structures Laboratory, Tokyo Institute of Technology, Yokohama 226-8503, Japan*
[b] *Laboratory of Inorganic and Analytical Chemistry, Helsinki University of Technology, FI-02015 TKK, Finland*
[c] *Physics Department, Åbo Akademi, FI-20500 Turku, Finland*

Received 1 August 2006; received in revised form 18 October 2006; accepted 31 October 2006
Available online 9 November 2006

Abstract

Substitution of divalent Sr by trivalent La is found to affect the valence states of both of the two *B*-site cations, Fe and Ta, in the double perovskite oxide $(Sr_{1-x}La_x)_2FeTaO_6$. Moreover, it improves the degree of order of these cations. From ^{57}Fe Mössbauer spectra the average Fe valence was found to decrease with increasing La substitution level, *x*. However, the valence of Fe decreased less than expected if the valence of Ta was assumed to remain constant. Hence, we conclude that also the valence of Ta decreases.

Keywords: Double-perovskite oxide; Cation valences; Cation ordering; Mössbauer spectroscopy

1. Introduction

An exciting family of complex perovskite oxides is derived from the ABO_3 perovskite structure upon co-occupation of the *B*-cation site by two different cation species, B' and B''. In the case of a *B*-site ordered double perovskite (BODP) equal amounts of cations B' and B'' occupy the *B* site in an ordered manner and the size of the unit cell is doubled along all the three crystal axes. Hence, an ideal BODP contains alternately $B'O_6$ and $B''O_6$ octahedra such that each $B'O_6$ octahedron is surrounded with six $B''O_6$ octahedra and vice versa. The tendency of the *B*-site cations to place themselves in an ordered manner depends strongly on the choice of the B' and B'' cations, and particularly on their valence states. Perfectly ordered compounds are typically achieved only for B'^{I}–B''^{VII} and B'^{II}–B''^{VI} combinations, whereas for the B'^{III}–B''^{V} configuration, various degrees of ordering are commonly seen. Apart from the mutual valence states, the synthesis conditions also play an important role [1,2].

The BODPs have attracted considerable attention after the discovery of half-metallic band structure and room-temperature tunneling-type magnetoresistance (TMR) effect in Sr_2FeMoO_6 [3]. In terms of the *B*-cation valence states, a so-called valence-mixing phenomenon is seen for Sr_2FeMoO_6 [4–7]: the itinerant *d* electron of formally pentavalent Mo ($4d^1$) transfers part of its charge and spin to formally trivalent Fe ($3d^5$) resulting in the mixed-valence states of $Fe^{II/III}$ and $Mo^{V/VI}$. It moreover seems that the occurrence of the valence-mixing phenomenon is strongly linked with the degree of ordering between the *B*-site cation constituents, such that in (partially) disordered samples the valence mixing is hindered [8]. Intensive chemical substitution studies at both *A* and *B* cation sites have yielded a whole family of half-metallic double perovskites, $A_2FeB''O_6$ (A = Ca, Sr, Ba; B'' = Mo, Re) [9,10]. These compounds exhibit as common characteristics both the valence-mixing phenomenon and high degrees of ordering among the *B*-site cations, Fe and Mo/Re [4–8,11,12].

Aliovalent substitutions (e.g., R^{III}-for-A^{II}; R = rare earth element) have been employed to control the properties of the BODPs [13,14]. Electron doping through

*Corresponding author. Laboratory of Inorganic and Analytical Chemistry, Helsinki University of Technology, P.O. Box 6100, FI-02015 TKK, Finland. Fax: +358 9 462 373.
E-mail address: Maarit.Karppinen@tkk.fi (M. Karppinen).

0022-4596/$ - see front matter © 2006 Elsevier Inc. All rights reserved.
doi:10.1016/j.jssc.2006.10.034

La^{III}-for-Sr^{II} substitution in Sr_2FeMoO_6 increases the Curie temperature but destroys the half-metallic behavior as a consequence of the decreasing degree of order (and valence mixing) [15–17]. For the $Sr_2Fe^{III}Ta^{V}O_6$ compound, in which the *B* cations Fe^{III} and Ta^{V} normally would not place themselves in an ordered manner, the effect was found to be opposite: electron doping increases the long-range order parameter [18]. In our previous work, X-ray absorption near-edge structure (XANES) spectroscopy measurements performed at both Fe *L* and Ta *L* edges were employed to demonstrate that electron doping in $(Sr,La)_2FeTaO_6$ lowers the (average) valence states of both Fe and Ta [18]. However, XANES spectroscopy does not show whether the nominal mixed-valency of the investigated metal cations results from a mixture of two distinct species of different integer valence values (e.g., Fe^{II} and Fe^{III}) or from true valence-mixing state (e.g., $Fe^{II/III}$) in which a fraction of charge density of one cation is transferred to another. In the present work, ^{57}Fe Mössbauer spectroscopy has been employed to more precisely investigate the nature of the *B*-cation valence states in $(Sr,La)_2FeTaO_6$.

2. Experimental

Two series of $(Sr_{1-x}La_x)_2FeTaO_6$ samples were employed with La substitution levels, x, of 0.0, 0.1, 0.2, 0.3 (Series A) and 0.0, 0.1, 0.2, 0.25, 0.3 (Series B). For sample synthesis, stoichiometric mixtures of high-purity (>99.9%) powders of $SrCO_3$, La_2O_3 (fired at 1000 °C before weighing), Fe_2O_3 and Ta_2O_5 were first calcined at 1000 °C for 24 h. Then the precursor was pelletized and sintered for 20–30 h in a high-temperature vacuum furnace at 1400 °C for Series A and at 1550 °C for Series B (with a slow cooling in more than 12 h in both cases). The former series comprises the samples investigated in Ref. [18] by means of XANES spectroscopy; the reason to prepare the latter series at a somewhat higher synthesis temperature was our aim to enhance the degree of *B*-cation ordering which for the samples of Series A had turned out to be considerably low [18].

The phase purity of the samples was confirmed by X-ray diffraction measurements (XRD; Rigaku 2500 V equipped with a rotating anode; CuK_α radiation). Lattice parameters and fractional *B*-cation occupancies were refined from the XRD data using the program RIETAN-2000 [19]. The degree of order was calculated from the fractional occupancy of Fe (g_{Fe}) at its correct crystallographic site as $S = 2(g_{Fe}-0.5)$. Hence for a completely ordered (disordered) sample, S receives a value of 1 (0).

Oxygen contents were analyzed by means of cerimetric titration for representative samples of the two sample series. Due to the poor sample solubility in diluted acids, the experiments were performed in a highly concentrated HCl solution [18]. Approximately 20 mg of fine sample powder was dissolved in 120 mL 9 M HCl solution in a sealed beaker under Ar flow. The dissolution was assisted with stirring and heating. After complete dissolution the beaker was immediately cooled to room temperature in an ice bath and the low-valent Fe and/or Ta species in the solution were then titrated (i.e., oxidized) with 0.008 M $Ce(SO_4)_2$ using ferroin as an indicator. The Ce^{4+} solution was standardized against Mohr's salt. The Fe^{3+} ions produced upon sample dissolution/during the course of titration were complexed with phosphoric acid to improve the visibility of the end-point. In order to take into account the unavoidable redox reaction between Cl^- and Fe^{3+} ions in concentrated HCl solutions, blank titrations were carried out employing exactly the same dissolution and titration procedure as used for the double-perovskite samples and utilizing Fe_2O_3 as the source for trivalent Fe. Each titration experiment was repeated at least three times with a reproducibility of ± 0.01 or better for the calculated oxygen content.

The Mössbauer spectra were collected in transmission geometry at room temperature. The absorber was made by mixing the sample powder in epoxy resin and spreading the mixture smoothly on an aluminum foil. The thickness of the sample material was approximately 35 mg/cm^2. A linear Doppler velocity sweeping from -3 to $+3$ mm/s was used. A Ritverc Company ^{57}Co:Rh (50 mCi, September 2003) source was used for producing the Mössbauer γ-quanta. The chemical isomer shift corresponding to α-Fe (IS), quadrupole coupling constant (eQV_{zz}), resonance linewidth (Γ) and the relative intensity of the component (I) were used as fit parameters in the analysis of the Mössbauer data. In order to improve the fitting a distribution was employed for the quadrupole coupling constant values. A Gaussian distribution was assumed and its width ΔeQV_{zz} was used as a common fit parameter for all spectral components.

3. Results and discussion

According to X-ray diffraction data, phase-pure samples of $(Sr_{1-x}La_x)_2FeTaO_6$ were obtained up to the La solubility limit of $x \approx 0.25$. For the $x = 0.3$ samples of both series a small (less than 1%) impurity appeared. In order to identify the impurity phase we prepared samples containing larger amounts of La. For these samples increasing amounts of La_3TaO_7 were detected. From the XRD data, structural parameters, including the lattice parameters and fractional Fe and Ta occupancies, were refined in the monoclinic space group $P2_1/n$ (#14) [18]. The obtained Rietveld refinement profile for the $x = 0.25$ sample of Series B is presented in Fig. 1; the magnification showing both supercell and fundamental reflections is to illustrate the similar width of these Bragg peaks. Arrows are used to indicate the superstructure reflections. With increasing x, the unit cell expands along all the three crystal axes, even though the size of the La^{III} ion is smaller than that of Sr^{II}, see Fig. 2. The increase in the cell volume is due to the electron-doping effect, which reduces the average valence of the *B* cations, thus increasing their ionic radii. In

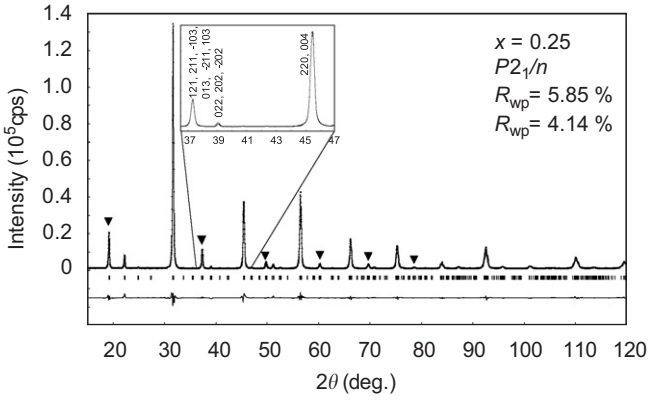

Fig. 1. Observed (dots) and calculated (solid line) room-temperature X-ray powder diffraction profiles for the Series B sample of $(Sr_{1-x}La_x)_2FeTaO_6$ with $x = 0.25$. The vertical lines indicate the positions of the allowed Bragg reflections. The difference curve, I_{obs}–I_{calc}, is shown at the bottom. The inset shows a magnification at $2\theta \approx 37$–47° to illustrate the similar width of the superstructure and fundamental reflections. The superstructure peaks are marked with arrows.

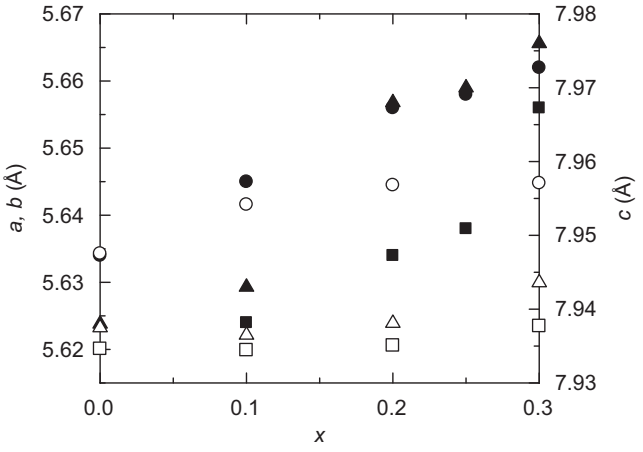

Fig. 2. Lattice parameters, a (■), b (●) and c (▲), for Series B samples of $(Sr_{1-x}La_x)_2FeTaO_6$ obtained from the Rietveld refinements and plotted against the La-substitution level, x. Corresponding open symbols are used to depict the lattice parameters for Series A samples.

Fig. 2, the data are somewhat scattered, especially for Series A. This is explained by the fact that the lattice parameters are simultaneously controlled by many competing factors, i.e., size difference between the A-site cations La^{III} and Sr^{II}, degree of B-cation order [1], and distribution of the doped electrons between Fe and Ta.

From the Rietveld refinement results for the fractional occupancies the long-range order parameter S was found to increase with the La substitution level, x, in both sample series. Synthesizing the sample at a higher temperature enhanced the ordering too: for samples of Series B notably higher S values were obtained compared with the corresponding samples of Series A. This is in line with earlier reports concluding that the degree of order in BODSs is mainly controlled by kinetics [1,2]. In addition, the Bragg reflections originating from the doubled unit cell

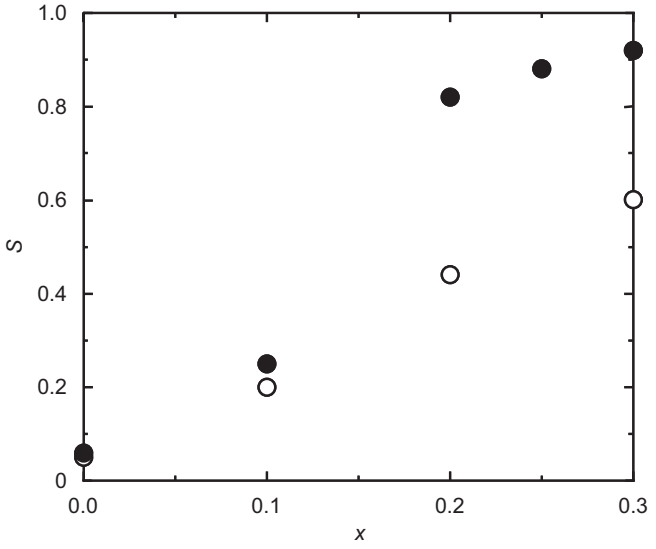

Fig. 3. Degree of order (S) plotted against La-substitution level (x) in $(Sr_{1-x}La_x)_2FeTaO_6$ samples. The data are for both Series A (open circles) and Series B (filled circles) samples.

were found to be as sharp as the fundamental reflections for Series B samples but not for Series A samples. Fig. 3 depicts the value of S against x for the two sample series, A and B.

The $x = 0.0$ and 0.2 samples of both series were investigated for the oxygen content by means of cerimetric titration analysis which yielded values very close to the stoichiometric value: 6.00 (5.96) and 6.00 (5.99) for $x = 0.0$ and 0.2 of Series A (Series B). The slightly lower values for the Series B samples in comparison to those of Series A are understandable since the samples were synthesized at a higher temperature. Also, the increase in oxygen content seen for Series B when the La content x was increased is what one expects upon trivalent-for-divalent cation substitution, i.e., partial compensation of the electron-doping effect.

The ^{57}Fe Mössbauer spectra (Fig. 4) obtained for the samples were analyzed using a maximum of three spectral components for both series. All components are described by doublet peaks in line with the paramagnetic nature of the samples at room temperature, found earlier from magnetization measurements [18]. Components belonging to the reduced state of Fe^{II} are readily observed owing to their high isomer shift, causing a characteristic shoulder to appear around $+1.0$ mm/s. The fitting results are summarized in Table 1. The non-substituted Sr_2FeTaO_6 sample of Series A (left panel in Fig. 4) contains Fe only at one valence state, i.e., Fe^{III}. Accordingly a symmetrical doublet having a small quadrupole effect is seen about $+0.4$ mm/s. Similar results for the pristine Sr_2FeTaO_6 compound have been reported earlier as well [20,21]. Presence of some quadrupole splitting is very typical and arises from the fact that the coordination polyhedra around Fe are not completely regular. The linewidth Γ is significantly broad. This is due to the random distribution of Fe^{III} and Ta^{V}

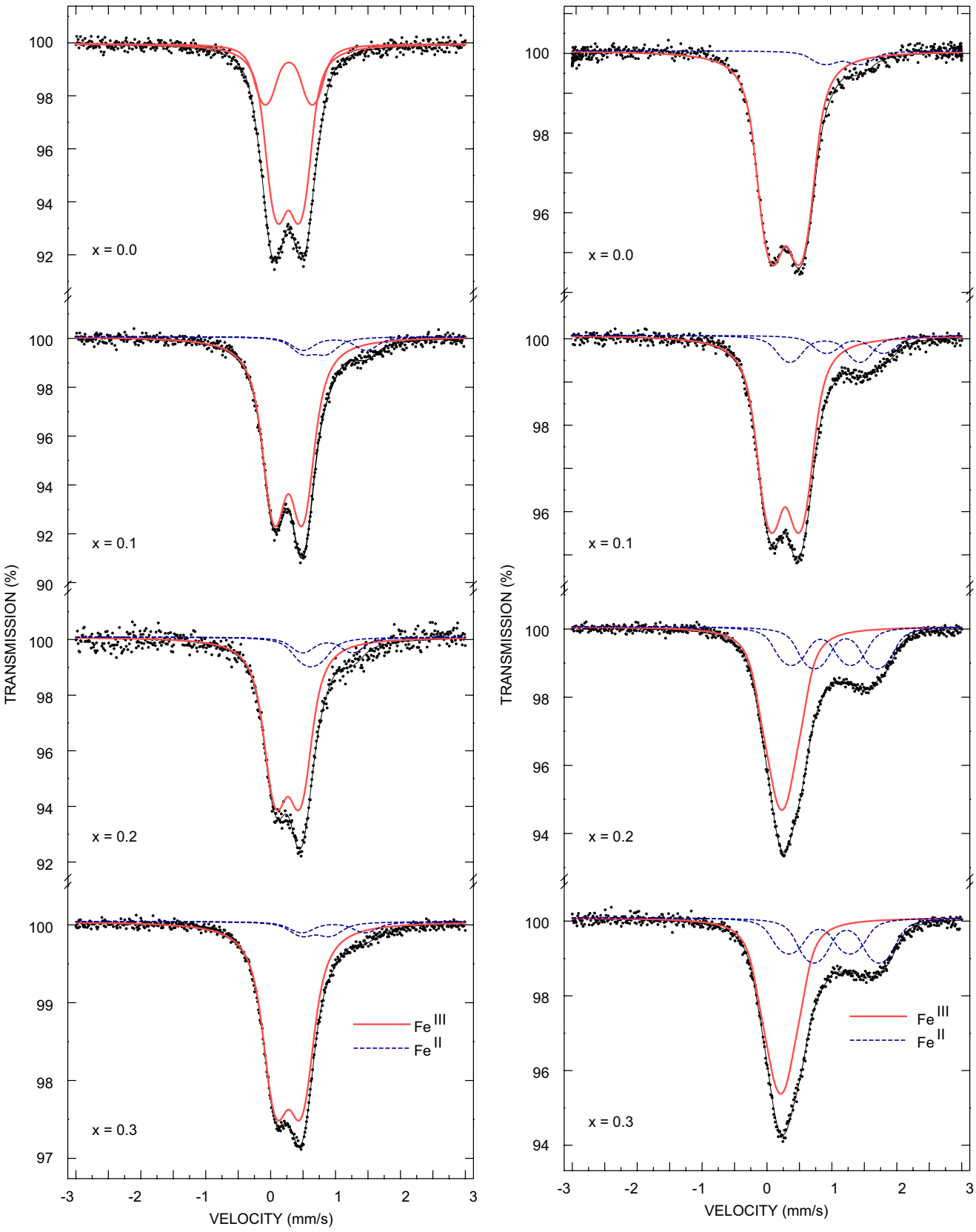

Fig. 4. ^{57}Fe Mössbauer spectra recorded at 300 K for Series A (left) and Series B (right). Components used in the fittings are displayed above the data. The component assignments are shown in the legends.

Table 1
Hyperfine parameters obtained for the $(Sr_{1-x}La_x)_2FeTaO_6$ samples from the computer fittings of ^{57}Fe Mössbauer spectra at room temperature

	x	Comp.	Fe Species	IS (mm/s)	$eQVzz$(mm/s)	I(%)
A	0.00	C1(a)	III	0.39	0.74	72.4
		C1(b)	III	0.39	1.46	27.6
	0.10	C1	III	0.38	0.89	85.2
		C2	II	0.79	0.72	7.8
		C3	II	1.10	1.96	7.0
	0.20	C1	III	0.38	0.78	80.7
		C2	II	0.73	0.51	10.9
		C3	II	0.99	1.54	8.5
	0.30	C1	III	0.39	0.78	87.3
		C2	II	0.81	0.51	6.9
		C3	II	1.08	1.54	5.8
B	0.00	C1	III	0.41	0.96	93.7
		C2	II	1.30	1.12	6.3
	0.10	C1	III	0.39	0.95	79.7
		C2	II	1.00	2.16	12.2
		C3	II	1.47	1.77	8.1
	0.20	C1	III	0.34	0.49	56.5
		C2	II	0.94	1.86	20.8
		C3	II	1.33	1.96	22.7
	0.25	C1	III	0.35	0.47	56.9
		C2	II	0.94	1.90	21.0
		C3	II	1.36	1.87	22.1
	0.30	C1	III	0.32	0.47	55.1
		C2	II	0.92	1.90	19.9
		C3	II	1.34	2.03	25.0

species in the samples, which effectively causes the local quadrupole coupling constant to vary. This type of widening makes it more difficult to obtain good fitting results for the spectrum. Therefore, to improve the fitting, we included a second component of similar IS value into the final fitting. The IS values of 0.38–0.39 mm/s obtained for the two sub-components, C1a and C1b, are typical for high-spin (HS) trivalent iron, Fe^{III}. For the $x = 0$ sample of Series B, a small shoulder located around $+1.0$ mm/s appears. This is due to divalent iron, Fe^{II}. However, the overall concentration of this species is only 6.3 % (Table 1), indicating an oxygen content of 5.97 per formula unit. The Mössbauer data for the $x = 0$ samples are in excellent agreement with the results of chemical analysis, showing stoichiometric oxygen content for the pristine sample of Series A and only minute oxygen deficiency for the pristine sample of Series B.

Upon electron doping by means of La^{III}-for-Sr^{II} substitution, the main doublet peak loses its symmetrical form even for the Series A samples (left panel of Fig. 4.) and can no longer be explained only with a single component. On the right-hand side of the main peak, the small shoulder appears. Again, it was fitted with a doublet with a large IS value originating from HS Fe^{II} (component C3, see Table 1). Moreover, the Fe^{III} region develops an asymmetry, which can be fitted with two spectral components: the original C1 corresponding to HS Fe^{III} component and component C2, which has an isomer shift which is notably higher than would be expected for trivalent Fe in this environment and rather low for HS Fe^{II}. Possibly it could be due to mixed-valence state of $Fe^{II/III}$. However, considering the low intensity of component C2 and the rather low overall concentration of reduced iron, we prefer to assign it to HS Fe^{II}. As the amount of La increases in the series, the total portion of components C2 and C3 increases at least up to $x = 0.2$ (Table 1).

The ^{57}Fe Mössbauer spectra of Series B samples, shown in Fig. 4 (right panel), differ somewhat from those of Series A. The decreased quadrupole coupling of the main component C1 (due Fe^{III}) is a consequence of the higher degree of order already seen in crystallographic examination. The significantly higher degree of order seems to cause higher symmetry around the FeO_6 octahedra. Surprisingly these samples contain much more of the Fe^{II} species than the corresponding Series A samples which is observed clearly even by visual interpretation of the Mössbauer spectra: the shoulder located around $+1.0$ mm/s has grown considerably in size. The shoulder was best fitted using two spectral components, both of which clearly belong to HS Fe^{II}. These "reduced" components are again denoted C2 and C3, although they do not exhibit quite the same hyperfine parameters as those observed for Series A. The enhanced concentration of Fe^{II} in the Series B samples most probably is not due to the presence of oxygen vacancies, as chemical analysis indicated that upon the La^{III}-for-Sr^{II} substitution the oxygen content rather increases.

The average valence states of the two *B*-site cations, Fe and Ta, can now be elucidated. Based on the XANES spectroscopy results, we previously proposed that the Ta atoms seem to also experience some reduction upon electron doping. Using the present Mössbauer results, we can revisit this topic. We calculate the average valence state of Fe in each sample from the fitted Mössbauer data using the relative intensities of the components from Table 1, and then the valence of Ta is obtained using the electroneutrality principle. For the Series B samples we have assumed an oxygen content of 5.97, as calculated for the $x = 0.0$ sample on the basis of Mössbauer data. Higher oxygen vacancy concentrations for the La-substituted samples are unlikely due to the "oxygen-content-increasing" influence of the La^{III}-for-Sr^{II} substitution. The calculated average valence states for Fe and Ta, denoted V(Fe) and V(Ta), are plotted in Fig. 5 against the La-substitution level, x. The result shows that electron doping through the La^{III}-for-Sr^{II} substitution has reduced the average valence of Fe but not enough to cover the stoichiometry in the system. Hence, we conclude that Ta is reduced as well. As the trend shows, reduction of Fe seems to be slowing down when approaching $x = 0.3$. This may be understood by the fact that the small impurity of La_3TaO_7 was seen for $x = 0.3$ which is consuming some of the lanthanum and therefore hinders its reductive effect on the $(Sr,La)_2FeTaO_6$ phase.

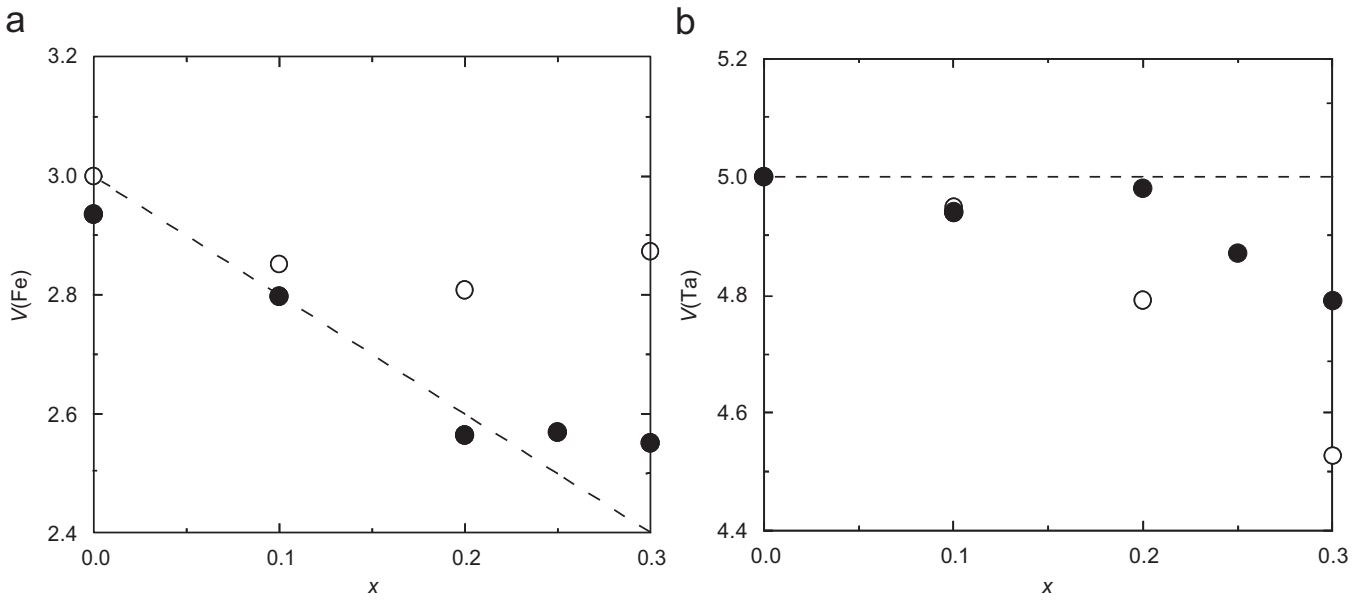

Fig. 5. Average valences of (a) iron [V(Fe)] and (b) tantalum [V(Ta)] in $(Sr_{1-x}La_x)_2FeTaO_6$ for both sample series, A (○) and B (●) with increasing x as estimated from the relative intensities of the different Mössbauer components (Table 1). The dashed lines illustrate the situation for V(Fe) and V(Ta), in which only Fe would be reduced.

4. Conclusions

Phase-pure samples of the electron-doped $(Sr_{1-x}La_x)_2FeTaO_6$ system were synthesized at two different temperatures by partially substituting La^{III} for Sr^{II}. The electron doping enabled the ordering of the *B*-site cations Fe and Ta, such that the samples adopted the double perovskite structure. Increasing the substitution level x and using higher synthesis temperatures enhanced the long-range ordering. ^{57}Fe Mössbauer spectroscopy measurements revealed presence of reduced Fe^{II} species and also indirectly indicated that not only Fe but also Ta is reduced upon the La^{III}-for-Sr^{II} substitution. In samples with higher degree of order, the reduction was found to be stronger for Fe than for Ta.

Acknowledgments

This work was supported by a Grant-in-aid for Scientific Research (no. 15206002) from Japan Society for the Promotion of Science, and also by Academy of Finland (Decision 110433). E.-L.R. acknowledges the support from Jenny and Antti Wihuri Foundation.

References

[1] P. Woodward, R.-D. Hoffmann, A.W. Sleight, J. Mater. Res. 9 (1994) 2118.
[2] T. Shimada, J. Nakamura, T. Motohashi, H. Yamauchi, M. Karppinen, Chem. Mater. 15 (2003) 4494;
Y.H. Huang, J. Lindén, H. Yamauchi, M. Karppinen, Chem. Mater. 16 (2004) 4337.
[3] K.-I. Kobayashi, T. Kimura, H. Sawada, K. Terakura, Y. Tokura, Nature 395 (1998) 677.
[4] J. Lindén, T. Yamamoto, M. Karppinen, H. Yamauchi, T. Pietari, Appl. Phys. Lett. 76 (2000) 2925.
[5] O. Chmaissem, R. Kruk, B. Dabrowski, D.E. Brown, X. Xiong, S. Kolesnik, J.D. Jorgensen, C.W. Kimball, Phys. Rev. B 62 (2000) 14197.
[6] J.M. Grenèche, M. Venkatesan, R. Suryanarayanan, J.M.D. Coey, Phys. Rev. B 63 (2001) 174403.
[7] M. Karppinen, H. Yamauchi, Y. Yasukawa, J. Lindén, T.S. Chan, R.S. Liu, J.M. Chen, Chem. Mater. 15 (2003) 4118.
[8] Y. Yasukawa, J. Lindén, T.S. Chan, R.S. Liu, H. Yamauchi, M. Karppinen, J. Solid State Chem. 177 (2004) 2655.
[9] K.-I. Kobayashi, T. Kimura, Y. Tomioka, H. Sawada, K. Terakura, Y. Tokura, Phys. Rev. B 59 (1999) 11159.
[10] A. Maignan, B. Raveau, C. Martin, M. Hervieu, J. Solid State Chem. 144 (1999) 224.
[11] J. Gopalakrishnan, A. Chattopadhyay, S.B. Ogale, T. Venkatesan, R.L. Greene, A.J. Millis, K. Ramesha, B. Hannoyer, G. Marest, Phys. Rev. B 62 (2000) 9538.
[12] J. Lindén, T. Yamamoto, J. Nakamura, H. Yamauchi, M. Karppinen, Phys. Rev. B 66 (2002) 184408.
[13] P.A. Ramakrishnan, U.V. Varadaraju, F.J. Berry, Mater. Lett. 38 (1999) 396.
[14] K. Ramesha, J. Gopalakrishnan, V. Smolyaninova, R.L. Greene, J. Solid State Chem. 162 (2001) 250.
[15] D. Sánchez, J.A. Alonso, M. García-Hernández, M.J. Martínez-Lope, M.T. Casais, J.L. Martínez, M.T. Fernández-Díaz, J. Magn. Magn. Mater. 272–276 (2004) 1732.
[16] C. Frontera, D. Rubí, J. Navarro, J.L. García-Muñoz, C. Ritter, J. Fontcuberta, Physica B 350 (2004) E285.
[17] J. Lindén, T. Shimada, T. Motohashi, H. Yamauchi, M. Karppinen, Solid State Commun. 129 (2004) 129.
[18] E.-L. Rautama, T.S. Chan, R.S. Liu, J.M. Chen, H. Yamauchi, M. Karppinen, J. Solid State Chem. 179 (2006) 111.
[19] F. Izumi, T. Ikeda, Mater. Sci. Forum 321–324 (2000) 198.
[20] P.D. Battle, T.C. Gibb, A.J. Herod, S.-H. Kim, P.H. Munns, J. Mater. Chem. 5 (1995) 865.
[21] J. Lindén, T. Yamamoto, J. Nakamura, H. Yamauchi, M. Karppinen, Phys. Rev. B 66 (2002) 184408.